Quaternary Research 74 (2010) 207–215

Contents lists available at ScienceDirect

Quaternary Research

journal homepage: www.elsevier.com/locate/yqres

Late second–early first millennium BC abrupt climate changes in coastal Syria and their possible significance for the history of the Eastern Mediterranean

D. Kaniewski [a,b,c,*], E. Paulissen [d], E. Van Campo [a,b], H. Weiss [e], T. Otto [a,b], J. Bretschneider [f], K. Van Lerberghe [f]

[a] Université de Toulouse, UPS, INPT, EcoLab (Laboratoire d'Ecologie Fonctionnelle), 29 rue Jeanne Marvig, 31055 Toulouse, France
[b] CNRS, EcoLab (Laboratoire d'Ecologie Fonctionnelle), 31055 Toulouse, France
[c] Center for Archaeological Sciences, Katholieke Universiteit Leuven, Celestijnenlaan 200E, 3001 Heverlee, Belgium
[d] Physical and Regional Geography Research Group, Katholieke Universiteit Leuven, Celestijnenlaan 200E, 3001 Heverlee, Belgium
[e] Department of Anthropology and Environmental Studies Program, Yale University, New Haven, CT 06520, USA
[f] Near Eastern Studies Unit, Katholieke Universiteit Leuven, Faculteit Letteren, Blijde-Inkomststraat 21, 3000 Leuven, Belgium

ARTICLE INFO

Article history:
Received 4 June 2009
Available online 4 August 2010

Keywords:
Abrupt climate change
Late Bronze Age collapse
Dark Age
Gibala-Tell Tweini
Ugarit kingdom
Syria

ABSTRACT

The alluvial deposits near Gibala-Tell Tweini provide a unique record of environmental history and food availability estimates covering the Late Bronze Age and the Early Iron Age. The refined pollen-derived climatic proxy suggests that drier climatic conditions occurred in the Mediterranean belt of Syria from the late 13th/early 12th centuries BC to the 9th century BC. This period corresponds with the time frame of the Late Bronze Age collapse and the subsequent Dark Age. The abrupt climate change at the end of the Late Bronze Age caused region-wide crop failures, leading towards socio-economic crises and unsustainability, forcing regional habitat-tracking. Archaeological data show that the first conflagration of Gibala occurred simultaneously with the destruction of the capital city Ugarit currently dated between 1194 and 1175 BC. Gibala redeveloped shortly after this destruction, with large-scale urbanization visible in two main architectural phases during the Early Iron Age I. The later Iron Age I city was destroyed during a second conflagration, which is radiocarbon-dated at *circa* 2950 cal yr BP. The data from Gibala-Tell Tweini provide evidence in support of the drought hypothesis as a triggering factor behind the Late Bronze Age collapse in the Eastern Mediterranean.

Introduction

Late Bronze Age (LBA) cities and states from Greece through Mesopotamia to Egypt declined or collapsed during the first quarter of the twelfth century BC (Carpenter, 1966; Brinkman, 1968; Weiss, 1982; Neumann and Parpola, 1987; Alpert and Neumann, 1989; Beckman, 2000). This sudden and culturally disruptive transition, termed LBA collapse (Weiss, 1982), is followed by the Dark Age (1200–825 BC) during which regional cultures are poorly documented (Weiss, 1982; Haggis, 1993; Chew, 2007). Regarding the possible cause of the LBA collapse, suggestions include destructions by outside forces (the Sea Peoples), climatic, environmental or natural disasters, technological innovations, internal collapses, system collapse and anthropological or sociological theories dealing with states of inequality and the resulting political struggle between centre and periphery (Weiss, 1982; Neumann and Parpola, 1987; Bryce, 2005; Killebrew, 2005; Gilboa, 2006–2007). No coherent explanation scheme is yet available. Climatic changes at 8.2, 5.2 and 4.2 cal ka BP are thought to punctuate and redirect cultural trajectories in late prehistoric–early historic Eastern Mediterranean and West Asia (Weiss et al., 1993; Weiss and Bradley, 2001; deMenocal, 2001; Staubwasser and Weiss, 2006). The drought hypothesis was first developed by Carpenter (1966) to explain the collapse of the Mycenaean civilization and further developed by Weiss (1982) for the disappearance of the LBA palatial civilization in the Eastern Mediterranean.

A thousand-year-long pollen–climate record from alluvial deposits around the ancient coastal city of Gibala (Bretschneider and Van Lerberghe, 2008), the southernmost town in the Ugarit kingdom situated near modern Jableh (Syria), indicates a climate instability and a severe drought episode at *ca.* 3125–2775 cal yr BP (computed ages based on intercept ages) (Kaniewski et al., 2008). The 2σ probability distribution of the ^{14}C dates obtained for the climatic event ranges between 3265 and 3000 cal yr BP for the onset of the drought and 2930–2765 cal yr BP for the termination (Table 1). This climate shift, centred on the 13th–9th centuries BC, is of major interest in Mediterranean and West Asian environments where dry farming agro-production, pastoral nomadism, and fishing were the primary or secondary subsistence systems. Reduced precipitation may lead rain-fed cereal agriculturalists to habitat-tracking when agro-innovations are not available (Lewis, 1987; Staubwasser and Weiss, 2006; Reuveny, 2007).

* Corresponding author. Université de Toulouse, UPS, INPT, EcoLab (Laboratoire d'Ecologie Fonctionnelle), 29 rue Jeanne Marvig, 31055 Toulouse, France. Fax: +33 5 62 26 99 99.
E-mail address: kaniewsk@cict.fr (D. Kaniewski).

0033-5894/$ – see front matter
doi:10.1016/j.yqres.2010.07.010

Table 1
Details of the ^{14}C age determinations for the core TW-1. All ages have been calibrated with IntCal04-Calib Rev 5.0.1.

Samples	Depth (cm)	Laboratory codes	Material	14C yr BP	2σ cal yr BP	1σ cal yr BP	Intercept cal yr BP
TWE04 EP35	395	Beta-229047	Charcoals	2750 ± 40	2950–2760	2870–2790	2850
TWE04 EP57	680	Beta-229048	Charcoals	2970 ± 40	3260–3000	3220–3070	3160
TWE04 EP73	755	Beta-229049	Charcoals	3710 ± 40	4150–3950	4100–3980	4030
TWE04 EP75	785	Beta-233430	Charcoals	3680 ± 40	4100–3900	4080–3970	4050

Here we present for the first time an advanced picture of landscape change for the LBA collapse and the Dark Age for the coastal Gibala-Tell Tweini site. We use geomorphology and a refined numerically derived climatic proxy, a pollen-derived record of food availability based on cultivated plants (mainly cereals with a background of grapevine, walnut, hazel, and olive), a second core with 3 new ^{14}C dates detailing the drought episode, and radiocarbon-dated archaeological data directly linked to the cultural changes in the Northern Levant during the period 1200–1000 BC. Environmental and archaeological data are used to test the hypothesis of the impact of fluctuating climate on food resources, eventually leading to famine, depopulation, migration, and on human ingenuity to face adverse environmental situations. The integration of both well-dated environmental and archaeological data along the Syrian coast suggests that explanations for the main changes affecting human life in the Eastern Mediterranean and West Asia during the LBA and Iron Age (IA) must consider the possible implications of climatic changes.

The site: Gibala-Tell Tweini

The Bronze Age Gibala (present Tell Tweini, 35°22′17.93″N, 35°56′12.60″E; elevation 19 to 27 meters above sea level; surface area 11.6 ha) (Fig. 1) is of major interest when studying the coastal town collapses in the northern Levant. This harbour town was occupied since the Early Bronze Age III–IV (*ca.* 2600 BC) and flourished during the Middle and Late Bronze Age. Commercial routes traversing the Jabal an Nuṣayrīyah (Alawite Mountains) connected Gibala with the Orontes Valley and Emar. The direct access from the Mediterranean to the Syrian heartland, Anatolia, and Mesopotamia was at the basis of the wealth of the ports of the Ugarit Kingdom. The term "Gi_5-bá-la" appears in the Akkadian tablets PRU 4, 71–76 and PRU 5, 74 (Bretschneider and Van Lerberghe, 2008).

The written LBA sources or epigraphic finds for Gibala cease as soon as Ugarit was destroyed. The city of Gibala is mentioned again during the IA II, in an inscription of Tiglatpileser III (744–727 BC). In the excavated areas of Gibala-Tell Tweini, the destruction layer, termed Level 7A, corresponds to the first conflagration of the city with the ruins of the LBA houses containing Late Helladic IIIB ceramics (1300–1190 BC). Level 7A represents the LBA collapse of Gibala nearly synchronous with the destruction of Ugarit, and other Northern Levantine coastal sites, such as Ras Ibn Hani, Ras el-Bassit, Tell Kazel, and Tell Sukas (Bretschneider and Van Lerberghe, 2008). Local Late Helladic IIIC Early ceramic is attested in Tell Tweini for the 12th century BC (Jung, 2010). The reuse of LBA ruins and the construction of new buildings indicate a local reoccupation since the very beginning of the Early IA (Level 6G–H, around the second half of the 12th century BC) (Bretschneider et al., 2010), as was also the case for some other secondary coastal sites such as Tell Kazel (Capet, 2003), Ras Ibn Hani and Ras el-Bassit (Caubet, 1989). For the remainder of the kingdom, the survival of place names for both large and small villages from the LBA to the present pleads in favour of some continuity in occupation (Yon, 1989).

A second architectural phase is attested at Gibala during the end of the Early IA I (Level 6E–F). The Level 6E (end of occupation), a 20–30 cm thick layer of powdery ashes, charcoals and charred seeds, represents the second conflagration. This level is located between earlier IA structures (Level 6G–H) and is directly covered by foundation walls belonging to Early IA II structures (Levels 6D–C) (Bretschneider et al., 2010). The city only re-flourished during the 9th and 8th centuries BC (IA II, Levels 6D–A).

Materials and methods

Cores geomorphology, lithology, and chronology

The data presented in this paper are based on two cores from the immediate vicinity of the pear-shaped Gibala-Tell Tweini (maximal dimensions: E–W: 350 m; N–S: 250 m). The TW-1 core (800 cm; 35°22′22.94″N, 35°56′12.49″E, 17 m a.s.l., 1.75 km from the Mediterranean) was retrieved from the thick alluvial deposits (bottom not reached) of the Rumailiah River. The core is situated just north of the Tell and just downstream of a pronounced river bend. TW-1 has been selected from a S–N core transect between the Tell foot and the river. Colluvial deposits at the Tell foot are very thin and are separated from the alluvial deposits by a 10-m section with the limestone bedrock at the surface. The alluvial deposits are aggraded in a former *ca.* 50-m-

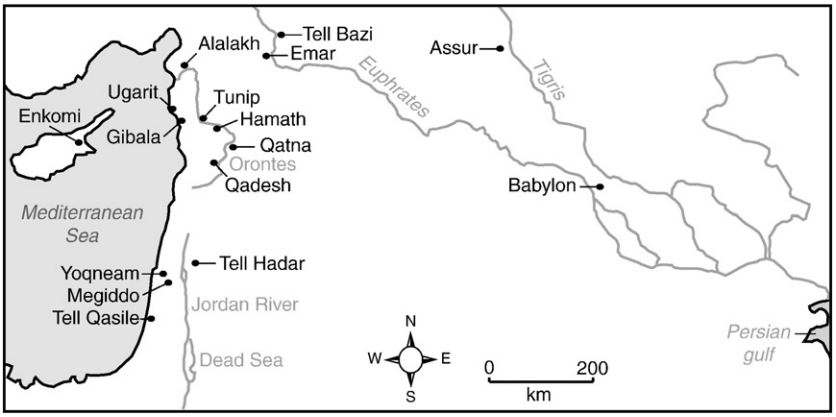

Figure 1. Near Eastern Mediterranean map with overview of some of the cities affected by the Late Bronze Age collapse and the "Dark Age". Cities are: Enkomi (Cyprus), Ugarit, Gibala-Tell Tweini, Tell Hadar, Yoqneam, Meggido, Tell Qasile (Levant), Alalakh, Tunip, Hamath, Qadesh (Orontes), Emar and Tell Bazi (Euphrates), Assur and Babylon (Mesopotamia).

wide valley delimited by 1–2 m high morphological scarps. The present Rumailiah River has eroded a 6-m-deep ravine in these deposits so that the top is largely fossilized and out of the reach of most inundations.

The TW-2 core (450 cm; 35°22′13.16″N, 35°56′11.36″E; 16.06 m a.s.l., 1.6 km from the Mediterranean) was sampled from the alluvial deposits (bottom very probably reached) of a small first order spring-fed river valley bordering the Tell towards the south (Ain Fawar). The core is situated in the middle of the actual floodplain, here 40 m wide. The spring valley belongs morphologically to the Rumailiah basin because the alluvial deposits of both valley systems are constrained by gravel deposits and merge seaward from Gibala-Tell Tweini. The confluence of both rivers is defunct as the spring-fed river has been diverted.

The TW-1 core was sampled with a percussion-driven end-filling ramguts corer (length 100 cm; Ø 7.5 cm), and the much softer sediments in the TW-2 with a manual guts corer (length 100 cm; Ø 3.0 cm). Deposits were retrieved in multiple drives, but no sediment was lost during coring operations. No potential gaps or unconformities were observed in the core logs and field data.

The TW-1 core chronology relies on four accelerator mass spectrometry (AMS) ^{14}C ages on charcoal at depths of 785 cm, 755 cm (both in 800–700 cm ramguts drive), 680 cm (in 600–700 cm drive), and 395 cm (in 360–440 cm drive) (Table 1). In the TW-1 core, datable plant remains are lacking from the sediment column, above core depth 395 cm, which has the conventional age 2750 ± 40 ^{14}C yr BP (Beta-229047) (Table 1).

The TW-2 core chronology is based on three AMS ^{14}C ages on charcoal at following depths: 448 cm (in 450–351 cm drive), 403 (in 450–351 cm drive), and 341 cm depth (in 275–351 cm drive) (Table 2). In the TW-2 core, a major hiatus occurs between 341 cm (2640 ± 40 ^{14}C yr BP; Beta-261721) and 315 cm (1170 ± 35 ^{14}C yr BP; Poz-28589) depth. The upper column, without shard fragments, is AMS ^{14}C dated as Middle Ages–Modern Era (not included).

The AMS dates in each core show an orderly relationship with depth and are therefore considered reliable. All radiocarbon ages are calibrated by IntCal04-Calib Rev 5.0.1 (Reimer et al., 2004).

Compaction corrected deposition rates have been computed between the intercepts of adjacent ^{14}C ages. Although any single value, neither the intercept nor any other calculation, adequately describes the complex shape of a radiocarbon probability density function (Telford et al., 2004), a single value has to be used to calculate the time scale for numerical analyses. The age of each sample was calculated by interpolation.

The cores TW-1 and TW-2 have been correlated using pollen and pollen-derived Biome (PdB) data and elevations a.s.l. of the fluvial deposits from the main and the affluent valley (Fig. 2).

Sedimentology

A total of 83 samples from cores TW-1 and TW-2 have been analyzed (Fig. S1) according to a flow chart previously described (Kaniewski et al., 2007). The grain-size distributions were subdivided into fractions with similar behaviour and shown as two matrices:

- clay and very fine silt (<7.8 μm), fine and medium silt (7.8–31.2 μm), coarse silt till medium sand (31.2–500 μm) and >500 μm volume fractions
- oxydables, carbonate and rest fractions.

The sediment deposits in the TW-1 and TW-2 cores consist of a potential continuous sedimentation of carbonate-rich clays, fine silt, and sand with sporadic gravel concentrations (Figs. 2 and S1).

Pollen

The same 83 samples from cores TW-1 and TW-2 were prepared for pollen analyses using standard palynological procedures. Pollen grains were counted under ×400 and ×1250 magnification using a Leitz microscope. Pollen frequencies (%) are based on the total pollen sum (average 400 pollen grains) excluding local hygrophytes and spores of non-vascular cryptogams (Fig. S2). The ratios of arboreal and non-arboreal pollen provide an estimate of the relative forest density (Fig. S2). Cultivated plants and cereals time-series have been plotted on the linear age-scale.

Pollen data have been converted into Plant Functional Types (PFT-s) and a pollen-derived biomization of the PFT-s has been elaborated (Prentice et al., 1996; Tarasov et al., 1998). Three semi-quantitative climatic indexes (SQCI-s) have also been computed from pollen data (Kaniewski et al., 2008). The process used to convert environmental data into climatic proxy has been here modified and includes now the PdB and SQCI time-series in the principal components analysis (PCA) numerical matrix. The refined data (Fig. 3) are described using the computed age-scale model based on the AMS ^{14}C intercepts.

Results

Environmental data

Sediment characteristics

The fluvial deposition has taken place in a 50-m-wide confined valley belonging to the Rumailiah River. The detail of the sediment characteristics in TW-1 core (Fig. S1) is highly different, with a major break at *ca.* 3150 cal yr BP. This is the result of the combination of the huge differences between the mean sedimentation rates, 0.8 mm yr^{-1} for the period *ca.* 3950–3150 cal yr BP versus 9.35 mm yr^{-1} for the period *ca.* 3150–2850 cal yr BP (and extrapolated until *ca.* 2450 cal yr BP). No clear lag deposits have been observed in the cores, suggesting non-erosive contacts. The sedimentological transition between the older and the younger units is situated in the samples with a calculated age *ca.* 3150–3050 yr cal BP, somewhat younger than the pollen-derived environmental changes. The differences between these two units are also reflected in the carbonate content (and inversely in the other detritic materials), which is significantly higher in the younger deposits. Also the overall percentage of oxydables is lower, especially after *ca.* 2750 cal yr BP.

Throughout the deposits, the fine fraction (<7.81 μm) is largely dominant. After *ca.* 3150–3050 yr cal BP the deposits become coarser, as evidenced by a decrease of the fraction 7.81–31.24 μm and increases of the fractions >31.24 μm. This is especially true during the drought event, which marks the highest influx of coarser sediments, interpreted as deposition by more floods. After *ca.* 2850 cal yr BP, the influx of fractions >500 μm is replaced by an influx of mainly finer sand (fraction 31.24–500 μm), which comes to an end at about 2750 cal yr BP. The subsequent period is characterized by a distinct lower content of oxydables and sharp fluctuations in the mineralogical content and the fractions >500 μm.

Table 2
Details of the ^{14}C age determinations for the core TW-2. All ages have been calibrated with IntCal04-Calib Rev 5.0.1.

Samples	Depth (cm)	Laboratory codes	Material	14C yr BP	2σ cal yr BP	1σ cal yr BP	Intercept cal yr BP
TWE08 EP63	341	Beta-261721	Charcoals	2640 ± 40	2845–2725	2780–2740	2750
TWE08 EP73	403	Beta-261722	Charcoals	2720 ± 40	2885–2755	2850–2780	2790
TWE08 EP81	448	Poz-28165	Charcoals	2810 ± 30	3000–2845	2950–2875	2920

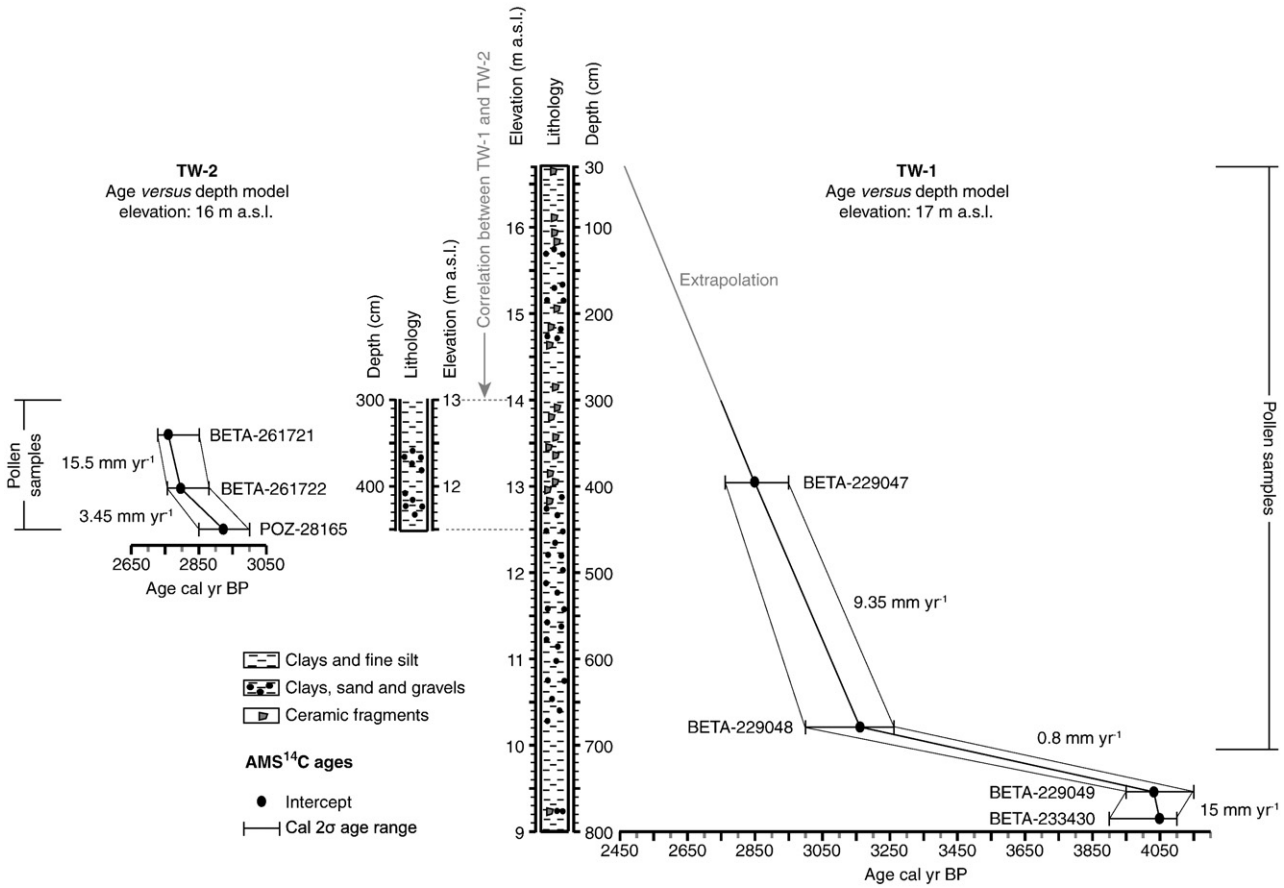

Figure 2. AMS ^{14}C calibrated ages and suggested age–depth curves. The correlation of the TW-1 and TW-2 cores is highlighted by dotted lines.

Pollen-derived climate record

The PCA-Axis 1 ordination of the TW-1 data accounts for most of the variance, with +.749 of total inertia (Figs. 3A and B). Arid/saline SQCI-s (+.1107), PdB Hot desert (+.6188), and PdB Warm steppe (+.2705) are loaded in positive values whereas negative values correspond to wet SQCI-s (−.5886), PdB Warm mixed forest (−.4067), and PdB Xerophytic woods/shrubs (−.047).

The refined pollen-based climate record shows moist climate conditions at *ca.* 3450–3150 cal yr BP, with a wetter pulse at *ca.* 3160 cal yr BP (Figs. 3A and B). The climatic instability starts abruptly at *ca.* 3150 cal yr BP and is characterized by increasing drought, peaking at *ca.* 2860 cal yr BP, but interrupted by a short wet pulse centred on *ca.* 2940–2920 cal yr BP. A pronounced wet peak at *ca.* 2775–2750 cal yr BP marks the abrupt end of the 350-yr drought event. A subsequent minor dry event, between *ca.* 2720 and 2675 cal yr BP (extrapolated age-scale), is followed by a *ca.* 125-yr-long gradually increasing wet phase until *ca.* 2550 cal yr BP. Relative frequencies of pollen indicators of crop cultivation and arboriculture (Fig. 3C) were considered as an indirect proxy of food availability. A straightforward relation is evidenced between drought phases and periods of low crop production, which could induce famines.

^{14}C age of destruction layer 6E

Three well-preserved charred botanical macro-remains retrieved *in situ* at two locations from ashes in Level 6E were AMS ^{14}C dated: from location 1, one olive stone (*Olea europaea*), and from location 2, two deciduous oak fragments, respectively from a branch 10 cm in diameter and from isolated charcoals degraded from the outer rings of this branch (Fig. 4, Table 3). These dates, with close conventional ages (Table 3), give an accurate chronology for this fire destruction of Gibala with a weighted average value (Bruins et al., 2003; Manning et al., 2006) of 2835 ± 20 ^{14}C yr BP (Fig. 4, Table 3). The IntCal04 calibration curve (Reimer et al., 2004) provides calibration ages of 2995–2875 cal yr BP (2σ, *probability* +1.0) and 2965–2945 cal yr BP (1σ, *probability* +0.7) with an intercept age of 2950 cal yr BP.

Discussion

Reliability of the age model

AMS ^{14}C ages 2970 ± 40 ^{14}C yr BP (Beta-229048) at 680-cm depth (13.09 m a.s.l.) and 2750 ± 40 ^{14}C yr BP (Beta-229047) at 395 cm in the TW-1 core are crucial as they date a 2.85-m sediment column deposited during about 300 yr, with a mean deposition rate of 9.35 mm yr^{-1} (Table 1; Fig. 2). The highly variable palynological composition (Fig. S2) and the intern variation in sediment characteristics (Fig. S1) provide evidence for a gradual deposition. These sediments are always completely different from the deposits below (Fig. S1).

The AMS ^{14}C age 2970 ± 40 ^{14}C yr BP (Beta-229048) (Table 1) dates the last peak of the wetter phase preceding the onset of the drought event (Fig. 3). Unfortunately, the shape and the wiggles in the calibration curve around 3150 cal yr BP have the effect of a plateau (Reimer et al., 2004) excluding a narrow resolution, even with several ^{14}C ages at the same level (Manning, 2006–2007). The ^{14}C age indeed shows large confidence limits with 3270–3000 cal yr BP at the 2σ level and 3220–3070 cal yr BP at the 1σ level (Table 1). This age range certainly puts the beginning of the climatic deterioration during a period covering the LBA IIB (1300–1200 BC) and the first half of the IA I (1200–900 BC).

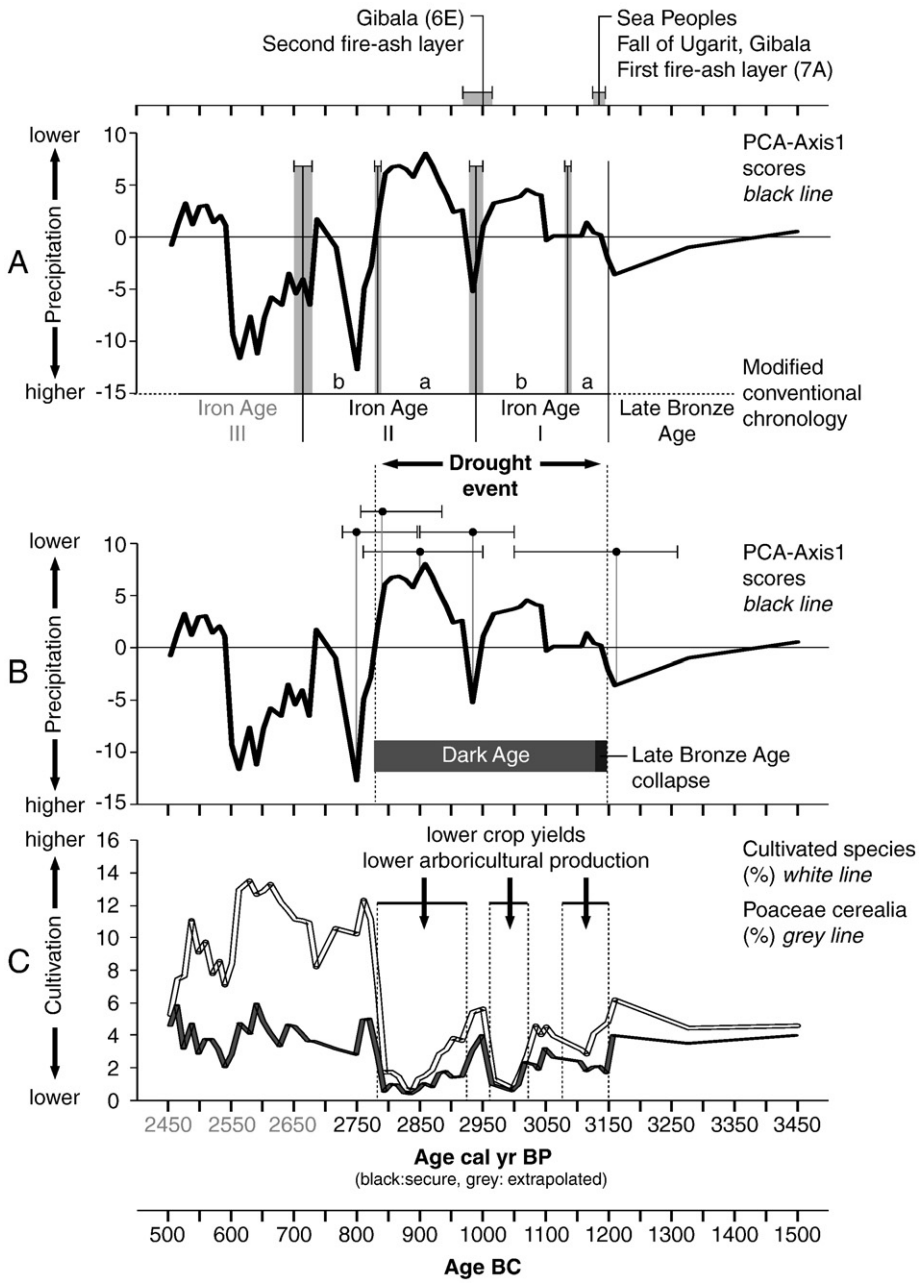

Figure 3. The Late Bronze Age collapse and Ancient Dark Age from the viewpoint of climatology and food availability. Shown is the LBA–IA sequence from the alluvial deposits of the Rumailiah River, north of Gibala-Tell Tweini. The pollen-derived climatic proxy is drawn as PCA-Axis 1 scores (A–B). The Late Bronze Age and Iron Age modified conventional chronology is shown with the PCA-Axis 1 scores (A). Grey shades indicate cultural changes. Cultivated species and Poaceae cerealia time-series are plotted on a linear age-scale (C). The main historical events are indicated at the top of the diagrams. Radiocarbon ages are displayed as 2σ calibration range. The black dots correspond to the intercepts with the calibration curve.

A tentative chronology of the sediment column above 395 cm in core TW-1 is based on the extrapolation of the deposition rate of 9.35 mm yr^{-1} from just below, suggesting an age of 2450 cal yr BP for the deposits at 30 cm below the surface (Fig. 3). The presence of a relative high number of weathered and nearly fresh IA shard fragments at different levels until the surface and the absence of more recent shards may confirm this IA age. It is believed that these shards are intercalated in the deposits during the fluvial aggradation process, but one can oppose that all these potteries may have been reworked. A (sub) recent or late historical age for the upper part of the alluvial deposits is excluded on morphological grounds because we have to take into account the time needed for the subsequent vertical erosion of the Rumailiah River, resulting in a 6-m-deep ravine in the coring area. The erosion of the main river is also reflected in the TW-2 core of the affluent valley by the erosion hiatus bracketed between the intercept ages 2750 cal yr BP (2640 ± 40 ^{14}C yr BP; Beta-261721) and 1065 cal yr BP (1170 ± 35 ^{14}C yr BP; Poz-28589). The latter sample is situated at 12.65 m a.s.l. and implies that at that time the Rumailiah River was at least situated at the same altitude, so that a ravine of at least 4 m existed already by then.

Focusing on the LBA collapse and the Dark Age, the AMS dates in each core show an orderly relationship with depth and are therefore considered reliable until *ca.* 2750 cal yr BP. The suggested connections for the period 2750–2450 cal yr BP (Fig. 3) are hypothetical.

Deteriorating climate during the late 13th/early 12th centuries BC

As a first approximation, the intercept age of 3160 cal yr BP can be used to date the beginning of the climatic deterioration. This intercept

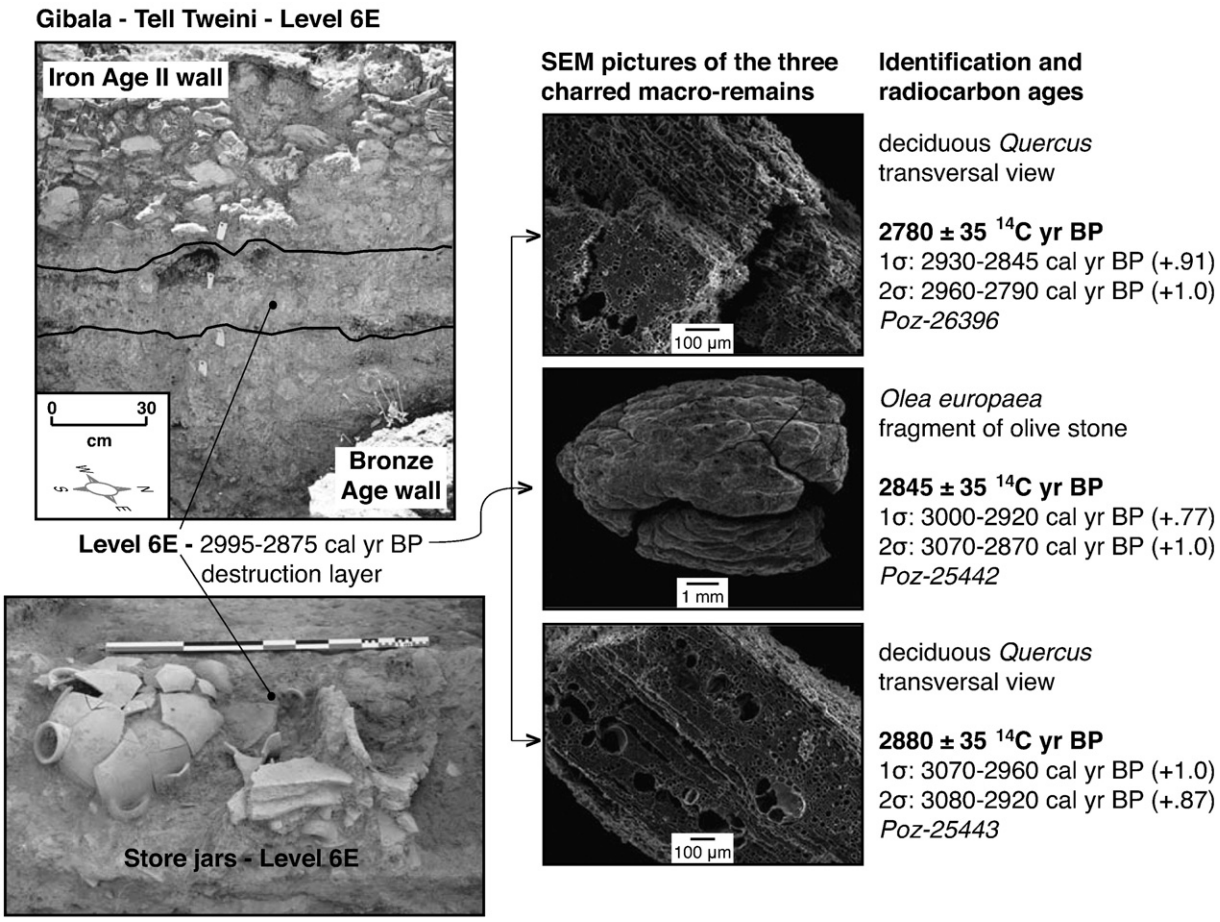

Figure 4. Radiocarbon dates of the destruction Level 6E, Gibala-Tell Tweini. The ages prove that the ash layer corresponds to the conflagration at the Iron Age I–II transition according to the Modified Conventional Chronology. The three charred macro-remains retrieved from the destruction layer are presented as scanning electron microscopy pictures with their respective radiocarbon ages and laboratory references. The scale for each macro-remain is indicated on the pictures. The radiocarbon dates are shown as ^{14}C yr BP, and 1σ and 2σ cal yr BP.

age corresponds with the generally accepted age for the collapse of the LBA cultures in the Eastern Mediterranean dated at *ca*. 1200 BC based on a complex integration from archaeological data and on literary sources, mainly from Ugarit. The northern Levantine Ugarit (Tell Ras Shamra), with its rich correspondence in the late 13th to early 12th centuries BC, is of main interest for the knowledge of the end of the LBA (Yon, 1989; Bryce, 2005), and the LBA collapse. Its harbours played a crucial role in grain shipments from Egypt and Canaan to Ura, the Hittite port on the coast of Cilicia in southern Anatolia. The chronological correspondence suggests a causal link between the climatic deterioration established in Mediterranean Syria, the decline in crop production and the LBA collapse, a theory already formulated by Carpenter (1966), Weiss (1982) and others. There are no written sources for these periods with direct information on climate or climate changes except the Aristotle's statement about the Mycenaean drought around 1200 BC (Neumann, 1985). Useful information is related to food production, grain shortages, famine, and Sea People migrations.

Near Eastern epigraphic and archaeological data document the invasions of the Sea Peoples (Yon, 2006; Gilboa, 2006–2007) and internal disintegration (Caubet, 1989) as the proximate cause for the LBA collapse in the northern Levant. The chronology of the Sea Peoples invasions is mainly based on letters just preceding the collapse of Ugarit (Yon, 1989; Singer, 1999; Dietrich and Loretz, 2002; Yon, 2006) and on Egyptian sources (Singer, 1999; Beckman, 2000). The Sea Peoples invasions were documented on the Ramses III's Medinet Habou Temple where they are illustrated with women and children suggesting movements of large kin-based units (Beckman, 2000). The fall of Ugarit is currently dated between 1194 and 1175 BC, between the terminus *post quem* supplied by the letter of the Egyptian Beya (1194–1186 BC) and the terminus *ante quem* of Ramses III's eight year (1175 BC) (Singer, 1999; Beckman, 2000). Freu (1988) concludes that tablet RS 86.2230 has been sent to Ugarit between 1197 and 1193 BC during the reign of Pharaoh Siptah and not during Sethnakht's reign, so that Ugarit has to be destroyed after 1195 BC and not before 1190 BC. A precise historical date of 1192–1185 BC is suggested by the combination of Ras Shamra clay tablet 86.2230 with the new dating of eclipse KTU 1.78 at 1192 BC (Dietrich and Loretz, 2002). The clay tablet RS 34.152, sent from Emar to Ugarit, is dated to *ca*. 1185 BC, before the fall of Emar at *ca*. 1175 BC (Cohen and d'Alfonso, 2008).

Table 3
Details of the ^{14}C age determinations for the Level 6E. All ages have been calibrated with IntCal04-Calib Rev 5.0.1.

Samples	Layer (Field A)	Laboratory codes	Material	14C yr BP	2σ cal yr BP	1σ cal yr BP	Intercept cal yr BP
TWE08 EP96	6E	Poz-26396	Charcoals	2780 ± 35	2960–2790	2930–2845	2890
TWE08 EP148	6E	Poz-25442	Olive stones	2845 ± 35	3070–2870	3000–2920	2960
TWE08 EP149	6E	Poz-25443	Charcoals	2880 ± 35	3080–2920	3070–2960	3010

Unfortunately, no absolute radiocarbon dates have been published for the destruction layer at Ugarit.

In coastal Syria, secure linkages between the LBA collapse and the onset of the drought event are particularly difficult to provide. The 3160 cal yr BP intercept is chronologically close to the 1194–1175 BC fall of Ugarit. The weak discrepancy between the written sources and the radiocarbon intercept may suggest that the drought event and the drought-induced decline in crop production start in the late 13th/early 12th centuries BC (Fig. 3C). Information from historical data that document episodes of food shortage in the Eastern Mediterranean, are rare. The clay tablet RS 34.152 from Emar is a vivid testimony to severe food shortage and to the deteriorating conditions in inner Syria around 1185 BC. The Emar year names bear witness to a staggering rise in grain prices in the "year of hardship/famine". Impoverished families were forced to sell their children to wealthy merchants in order to sustain themselves (Singer, 2000; Cohen and Singer, 2006). The clay tablet RS 18.38, dated from the late 13th century BC, indicates grain shipments from Egypt to the Hittites, suggesting grain shortages in Eastern Anatolia (Bryce, 2005). A particular note of urgency occurs in a letter sent from the Hittite court to the Ugaritic king, either Niqmaddu III (1210–1200 BC) or Hammurabi (1200–1194/1175), demanding ship and crew for the transport of 2000 kor of grain (*ca.* 450 tons) from the Syrian coastal district Mukish to Ura. The letter ended by stating that it is a matter of life or death (tablet RS 20.212) (Nougayrol et al., 1968). In Egypt, a famine struck the country during the reign of Merneptah (1213–1203 BC) (Bryson et al., 1974). The drop of Nile discharges during the reign of Ramses III (1186–1153 BC) has led to crop failures/low harvests (Butzer, 1976) and riots (Faulkner, 1975).

It is worth mentioning that Hatti may have very probably come to rely on grain importation during the last century of the Kingdom. Following the 1259 BC treaty between Ramses II and Hattusili III, grain was probably imported from Egypt into Anatolia on a regular basis (Bryce, 2005). This could indicate that even during the LBA humid climatic conditions (Fig. 3B), the Hatti Kingdom was no longer self-sustainable in food procurement and had to rely on food import. At the end of the 13th century BC, Pharaoh Merneptah (1213–1203 BC) sent to the Hittites the earliest known shipment of grain in the form of famine aid (Warburton, 2003; Bryce, 2005). The Hittite king Amuwanda III described the terrible hunger suffered during his father's day in Anatolia and mentioned drought as the reason (Warburton, 2003).

This evidence for the crises during the late 13th/early 12th centuries BC in the Eastern Mediterranean may serve as anchor points between the historical sources and the radiocarbon-dated decline in crop production in coastal Syria (Fig. 3C). The data suggest that the fall of Ugarit and secondary cities has to be placed within the drought period which may have started at the end of the 13th century BC. Inhabitants of the destroyed and abandoned LBA cities probably sought refuge in the mountain villages which were somewhat protected by being located away from the coast (Caubet, 1989; Yon, 1989). The fact that certain village names have been preserved from the LBA to the present leads these authors to believe that the village communities managed to survive, thanks to their inland location away from the coast.

A causal process for the northern coastal Levant migration might also have been the transient ameliorating effect of moister conditions on crop and food resources, concentrating population movement from the coast toward more fertile areas such as the riparian and adjacent karst aquifer-related settlements/cities of the Orontes River. The Sea Peoples may have induced the fall of the coastal Ugarit (1194–1175 BC), Ras Ibn Hani, Ras el-Bassit, Tell Kazel, Tell Sukas, and Gibala (Level 7A) followed by the destruction of several cities of the Hittite Empire (Tarsus, Hattusas) (Beckman, 2000), near the Orontes River (Alalakh, Tunip, Hamath, Qadesh) (Fugmann, 1958; Woolley, 1958; Bartl and al-Maqdissi, 2007; Whincop, 2007), and near the Euphrates (Emar, Tell Bazi, Tell Faq'us, Tell Fray, Tell Suyuh) (Adamthwaite, 2001; Beyer, 2001; Otto, 2007; Cohen, 2009) (Fig. 1).

The Dark Age

The duration of the drought event in coastal Syria has been estimated by a series of AMS ^{14}C dates obtained in the two cores, TW-1 (Table 1) and TW-2 (Table 2). Their ages range from the 13th/12th centuries BC until 9th/8th centuries BC. The AMS ^{14}C date for the basal sample in the TW-2 core (Fig. 2) gives an age of 2810 ± 30 ^{14}C yr BP (Poz-28165), with a 2σ confidence of 3000–2845 cal yr BP (intercept at 2920 cal yr BP) (Table 2). The second AMS ^{14}C age for the drought event has been obtained for the higher peak in the PCA-Axis1 curve (Fig. 3) and dated at 2750 ± 40 ^{14}C yr BP (Beta-229047) with a 2σ confidence of 2950–2760 cal yr BP (intercept at 2850 cal yr BP) (Table 1). The end of the drought event is enclosed in an interval between 2720 ± 40 ^{14}C yr BP (Beta-261722) and 2640 ± 30 ^{14}C yr BP (Beta-261721). In this interval, defined by a 2σ confidence of, respectively, 2885–2755 cal yr BP (intercept at 2790 cal yr BP) and 2845–2725 cal yr BP (intercept at 2750 cal yr BP) (Table 2), the drought suddenly ends. The TW-1 and TW-2 cores are consistent with a termination of the drought event during the 9th century, between 2790 and 2750 cal yr BP according to the intercepts. Archaeological data in coastal Syria show that dense occupation reappears during the end of the 9th or the 8th century BC (Caubet, 1989). The IA IIa–b transition is dated at 825 BC according to the Modified Conventional Chronology (MCC) (Mazar, 2005; Mazar and Bronk Ramsey, 2008). This transition is close to the intercept date at which the Dark Age ended in coastal Syria. Egyptian, Aegean, and Assyrian empires recovered with diversified agro-production (manna ash, olive tree, vine tree, walnut tree), pastoral activities, and sustained a cultural revival (Weiss, 1982). The archaeologically defined end of the Dark Age and the radiocarbon-dated end of the drought event are concordant in time.

The major environmental shift, interpreted as a result of lower amounts of precipitation in the Syrian coastal area (Figs. 3A and B) since 2970 ± 40 ^{14}C yr BP (Beta-229048), is synchronous with a dry southern basin and a low lake level in the northern basin for the Dead Sea (Bookman et al., 2004). The lowest value of the northern lake was reached at 3350 cal yr BP, before the onset of the Syrian climatic shift, and the level stays low throughout the drought event. The change in rainfall inducing a shortage of water supply in coastal Syria is derived from a synthesis of regional palaeoenvironmental proxy data, taking into account climatic signals and the temporal resolution represented in the records also correlated with *minima* in the Tigris and Euphrates river discharges from 1150 to 950 BC (Kay and Johnson, 1981; Neumann and Parpola, 1987; Alpert and Neumann, 1989), and with higher δ^{18}O values in the Ashdod coast record (Schilman et al., 2001, 2002). During this period, the Babylonian and Assyrian empires go into decline between 1200 and 900 BC (Brinkman, 1968; Neumann and Parpola, 1987). Written sources from Babylon mention crop failures, famine, outbreak of plague and repeated nomad incursions at that time (Neumann and Parpola, 1987). The historically defined Dark Age (1200–825 BC) (Weiss, 1982; Haggis, 1993) is synchronous with the period of drought and diminishing crop production (Fig. 3C) documented here.

Several not mutually exclusive mechanisms have been considered to explain the late Holocene centennial-scale climate variability, among which solar forcing (Versteegh, 2005) and ocean circulation changes (Bond et al., 2001) are plausible candidates. A comparison of the δ^{14}C solar proxy with the pollen-derived climatic proxy reveals a good correspondence between lowest atmospheric δ^{14}C values indicative of higher solar irradiance and the 350-yr drought event. These results suggest that middle-to-late Holocene precipitation changes over the Near East are associated with solar variability. Centennial–millennial droughts in the Eastern Mediterranean were also related to cooling periods in the North Atlantic for the past 55 ka BP (Bartov et al., 2003). A correspondence between the drought event in coastal Syria and the second peak of Bond event 2, identified in

North Atlantic core MC52-V29-191 by the bimodal increase of ice-rafted hematite stained grains, would confirm the role of the North Atlantic in modulating the Eastern Mediterranean climate at the centennial scale.

The destructions of Gibala-Tell Tweini

The first conflagration of Gibala has destroyed the LBA city. The corresponding destruction Level 7A contains typical Late Helladic IIIB ceramics. The destruction of this southernmost harbour town of the Ugarit Kingdom shows no discrepancy with Ugarit, which has been set ablaze at the LBA–IA transition.

The destruction of occupation Level 6E marks the second conflagration of Gibala (Fig. 4) and occurs at the MCC IA I–II transition, after *ca.* 2 centuries of drought and harvest failures (Figs. 3B and C). This conflagration Level contains typical store jars well preserved in room context, typologically dated in the 11th century BC (Fig. 4). In Level 6E, and also in the older Levels 6F–G–H, LBA potteries, characteristic for Levels 7A–B–C are absent, as well as typical forms, which appearing later in the IA II Levels 6C–D (Vansteenhuyse, 2010).

For the end of the Early IA I, major destruction levels are attested at Megiddo (2990–2880 cal yr BP), Yoqne'am (2995–2880 cal yr BP), Tell Qasile (3000–2890 cal yr BP), and Tell Hadar (3005–2880 cal yr BP) (Mazar and Bronk Ramsey, 2008) (Fig. 1). These southern Levantine sites correspond to flourishing, wealthy cities and settlements that were destroyed by violent conflagrations. The radiocarbon age of the destruction Level 6E at Gibala (2σ 3000–2870 cal yr BP) is close to the AMS ^{14}C age obtained at the bottom of the TW-2 core (3000–2845 cal yr BP), which dates a high accumulation of charred plant remains. The conflagration of the site and the charred remains in the TW-2 core may indicate a direct ^{14}C link between the archaeological and the environmental data at Gibala. This would suggest that the second conflagration of Gibala, with the destruction of the later IA I urbanization (Level 6E–F), is linked to the humid episode (Fig. 3). During the highest peak of drought, an occupation of low density is so far known from the site and crop production is at its minimum. Gibala clearly re-flourished during the 9th century BC.

The reasons behind the second destruction of Gibala are unknown. A first hypothesis may concern a second phase of migration following the same west–east axis comparable to the first wave, causing the conflagration of the re-occupied coastal towns. These climate-induced migrations since the end of the LBA would suggest that populations abandoned drought-stressed areas and tracked towards new more favorable environments. These repeated nomad incursions from the west were clearly identified at Babylon (Neumann and Parpola, 1987). In costal Syria, the hypothesis of a second wave of migration is not supported by archaeological proof. The second hypothesis of an earthquake around 1000 BC that may have destroyed Gibala is also not supported by any geological evidence in coastal Syria (Reida Sbeinati et al., 2005). Earthquake storms in the Aegean and Eastern Mediterranean have been only suggested for the late 13th/12th century crisis, not for later periods (Nur and Cline, 2000).

Conclusion

The integrated palaeoenvironmental and archaeological records from the Syrian coast suggests that climate shift may have been one of the causes behind the LBA collapse and the beginning of the IA. The Gibala-Tell Tweini data bring new hypotheses on the complex interactions between abrupt, high-magnitude, sustained Holocene climate change and social adaptations across time, space and socio-economic contingencies (deMenocal, 2001; Staubwasser and Weiss, 2006). Gibala is also a rare settlement, alongside Tell Kazel, Ras Ibn Hani and Ras el-Bassit, with Early IA I settlement after the LBA collapse. The Rumailiah River and the Ain Fawar spring-complex provided a stable water supply for resettlement on the surrounding alluvial plain despite climate shifts and successive destructions during the following Dark Age. Gibala also shows that there was no systematic one way reaction of the people regarding adverse environmental situations. At the late 13th/early 12th centuries BC period, the climate change may have induced cultural collapse. During the IA I and II, people were able to cope with the adverse situations. Moreover, past patterns of cultural responses to climate variability do not predict political and socio-economic impacts of future climate changes. They require, however, evaluating each abrupt climate change with contemporaneous social and political contingencies, and adaptive possibilities (Lewis, 1987; Reuveny, 2007).

Acknowledgments

This research is funded by the Fonds voor Wetenschappelijk Onderzoek, the Onderzoeksfonds Katholieke Universiteit Leuven, the Inter-university Attraction Poles Programme VI/34, Belgian Science Policy, Belgium, by the Paul Sabatier-Toulouse3 University, and the MISTRAL, INSU-CNRS Paleo2 MEDORIANT program. We wish to thank the Senior Editor, Professor Derek Booth, the Associate Editor, Professor Curtis W. Marean, and the three anonymous reviewers for their critical remarks and useful recommendations.

Appendix A. Supplementary data

Supplementary data associated with this article can be found, in the online version, at doi:10.1016/j.yqres.2010.07.010.

References

Adamthwaite, M.R., 2001. Late Hittite Emar. The Chronology, Synchronisms, and Socio-Political Aspects of a Late Bronze Age Fortress Town. : Ancient Near Eastern Studies Supplement Series, Vol. 8. Peeters, Leuven.
Alpert, P., Neumann, J., 1989. An ancient correlation between streamflow and distant rainfall in the Near East. Journal of Near Eastern Studies 48, 313–314.
Bartl, K., al-Maqdissi, M., 2007. Ancient settlements in the middle Orontes region between ar-Rastan and Qalcat Shayzar. First results of archaeological surface investigations 2003-2004. In: Morandi Bonacossi, D. (Ed.), Studi archeologici su Qatna. : Qatna, Vol. 1. Eisenbrauns, Udine, pp. 243–252.
Bartov, Y., Goldstein, S.L., Stein, M., Enzel, Y., 2003. Catastrophic arid episodes in the Eastern Mediterranean linked with the North Atlantic Heinrich events. Geology 31, 439–442.
Beckman, G., 2000. Hittite chronology. Akkadica 119–120, 19–32.
Beyer, D., 2001. Emar IV, Les sceaux. OBO Series Archaeologica, 20. Vandenhoeck & Ruprecht, Göttingen.
Bond, G., Kromer, B., Beer, J., Muscheler, R., Evans, M.N., Showers, W., Hoffman, S., Lotti-Bond, R., Hajdas, I., Bonani, G., 2001. Persistent solar influence on North Atlantic climate during the Holocene. Science 294, 2130–2136.
Bookman (Ken-Tor), R., Enzel, Y., Agnon, A., Stein, M., 2004. Late Holocene lake levels of the Dead Sea. Geological Society of America Bulletin 116, 555–571.
Bretschneider, J., Van Lerberghe, K., 2008. Tell Tweini, ancient Gibala, between 2600 BCE and 333 BCE. In: Bretschneider, J., Van Lerberghe, K. (Eds.), In Search of Gibala, an archaeological and historical study based on eight seasons of excavations at Tell Tweini (1999–2007) in the A and C fields. Aula Orientalis, Barcelona, pp. 12–66.
Bretschneider, J., Jans, G., Van Vyve, A.S., 2010. Les campagnes des Fouilles de 2009 et 2010. In: Al-Maqdissi, M., Van Lerberghe, K., Bretschneider, J., Badawi, M. (Eds.), Tell Tweini: onze campagnes de fouilles syro-belges (1999–2010). Documents d'Archéologie Syrienne, Damas. In Print.
Brinkman, J.A., 1968. A political history of post-Kassite Babylonia, 1158–722 BC. Analecta Orientalia, Ville.
Bruins, H.J., van der Plicht, J., Mazar, A., 2003. ^{14}C dates from Tel Rehov: Iron-Age chronology, Pharaohs and Hebrew Kings. Science 300, 315–318.
Bryce, T., 2005. The Kingdom of the Hittites. Oxford University Press, Oxford.
Bryson, R.A., Lamb, H.H., Donley, D., 1974. Drought and the decline of the Mycenae. Antiquity 43, 46–50.
Butzer, K.W., 1976. Early hydraulic civilization in Egypt. University of Chicago Press, Chicago and London.
Capet, E., 2003. Tell Kazel (Syrie), Rapport préliminaire sur les 9ème–17ème campagnes de fouilles (1993–2001) du Musée de l'Université Américaine de Beyrouth, Chantier II. Berytus 47, 63–121.
Carpenter, R., 1966. Discontinuity in Greek Civilization. Cambridge University Press, Cambridge.
Caubet, A., 1989. Reoccupation of the Syrian coast after the destruction of the "Crisis Years". In: Ward, W.A., Sharp Joukowsky, M. (Eds.), The Crisis years: the 12th century BC. From Beyond the Danube to the Tigris. Kendall/Hunt Publishing Company, Dubuque, pp. 123–131.

Chew, S.C., 2007. The recurring Dark Ages. Ecological stress, climate changes, and system transformation. Altamira Press, Lanham.
Cohen, Y., 2009. The scribes and scholars of the city of Emar in the Late Bronze Age. Harvard Semitic Studies, 59. Eisenbrauns, Winona Lake.
Cohen, Y., d'Alfonso, L., 2008. The duration of the Emar archives and the relative and absolute chronology of the City. In: d'Alfonso, L., Cohen, Y., Sürenhagen, D. (Eds.), The City of Emar among the Late Bronze Age Empires. History, landscape, and society. Proceedings of the Konstanz Emar Conference (2006). : Ugarit, Alter Orient und Altes Testament, Vol. 349. Münster, pp. 3–24.
Cohen, Y., Singer, I., 2006. Late Synchronism between Ugarit and Emar. In: Amit, Y., Zvi, E.B., Finkelstein, I., Lipschits, O. (Eds.), Essays on Ancient Israel in its Near Eastern Context. A Tribute to Nadav Na'ama. Eisenbrauns, Winona Lake, pp. 123–139.
deMenocal, P.B., 2001. Cultural responses to climatic change during the late Holocene. Science 292, 667–673.
Dietrich, M., Loretz, O., 2002. Der Untergang von Ugarit am 21. Januar 1192 v. Chn? Der astronomisch-hepatoskopische Bericht KTU 1.78 (RS 12.061). Ugarit-Forschungen 34, 53–74.
Faulkner, R.O., 1975. Egypt, from the inception of the nineteenth Dynasty to the death of Ramesses III. Cambridge Ancient History, Cambridge.
Freu, J., 1988. La tablette RS 86.2233 et la phase finale du Royaume d'Ugarit. Syria 65, 395–398.
Fugmann, E., 1958. Hama. Fouilles et recherches, 1931–1938. Carlsbergfondet, Copenhagen.
Gilboa, A., 2006–2007. Fragmenting the sea peoples, with an emphasis on Cyprus, Syria and Egypt: a Tel Dor perspective. Scripta Mediterranea 27–28, 209–244.
Haggis, D.C., 1993. Intensive survey, traditional settlement patterns and Dark Age Crete: the case of Early Iron Age Kavousi. Journal of Mediterranean Archaeology 6, 131–174.
Jung, R., 2010. La céramique de typologie mycénienne de Tell Tweini. In: Al-Maqdissi, M., Van Lerberghe, K., Bretschneider, J., Badawi, M. (Eds.), Tell Tweini: onze campagnes de fouilles syro-belges (1999–2010). Documents d'Archéologie Syrienne, Damas. In Print.
Kaniewski, D., Paulissen, E., De Laet, V., Dossche, K., Waelkens, M., 2007. A high-resolution Late Holocene landscape ecological history inferred from an intramontane basin in the Western Taurus Mountains, Turkey. Quaternary Science Reviews 26, 2201–2218.
Kaniewski, D., Paulissen, E., Van Campo, E., Al-Maqdissi, M., Bretschneider, J., Van Lerberghe, K., 2008. Middle East coastal ecosystem response to middle-to-late Holocene abrupt climate changes. Proceedings of the National Academy of Sciences of the United States of America 105, 13941–13946.
Kay, P.A., Johnson, D.L., 1981. Estimation of the Tigris–Euphrates streamflow from regional palaeoenvironmental proxy data. Climatic Change 3, 251–263.
Killebrew, A.E., 2005. Biblical peoples and ethnicity. An archaeological study of Egyptians, Canaanites, Philistines and Early Israel 1300–1100 BCE. Society of Biblical Literature, Archaeology, and Biblical Studies, Atlanta.
Lewis, N.N., 1987. Nomads and settlers in Syria and Jordan, 1800–1980. Cambridge University Press, Cambridge.
Manning, S.W., 2006–2007. Why radiocarbon dating 1200 BCE is difficult: a sidelight on dating the end of the Late Bronze Age and the contrarian contribution. Scripta Mediterranea 27–28, 53–80.
Manning, S.W., Bronk Ramsey, C., Kutschera, W., Higham, T., Kromer, B., Steier, P., Wild, E.M., 2006. Chronology for the Aegean Late Bronze Age 1700–1400 B.C. Science 312, 565–569.
Mazar, A., 2005. The debate over the chronology of the Iron Age in the Southern Levant. In: Levy, T., Higham, T. (Eds.), The Bible and Radiocarbon Dating: Archaeology, Text and Science. Equinox, London, pp. 15–30.
Mazar, A., Bronk Ramsey, C., 2008. ^{14}C dates and the Iron Age chronology of Israel: a response. Radiocarbon 50, 159–180.
Neumann, J., 1985. Climate change as a topic in the classical Greek and Roman literature. Climate Change 7, 441–454.
Neumann, J., Parpola, S., 1987. Climatic change and the eleventh-tenth-century eclipse of Assyria and Babylonia. Journal of Near Eastern Studies 46, 161–182.
Nougayrol, J., Laroche, E., Virolleaud, C., Schaeffer, C., 1968. Ugaritica V, Nouveaux textes accadiens, hourrites et ugaritiques des archives et bibliothèques privées d'Ugarit. Mission de Ras Shamra, 16. Librairie Orientaliste Paul Geuthner, Paris.
Nur, A., Cline, E.H., 2000. Poseidon's Horses: plate tectonics and earthquake storms in the Late Bronze Age Aegean and Eastern Mediterranean. Journal of Archaeological Science 27, 43–63.
Otto, A., 2007. Alltag und gesellschaft zur spaetbronzezeit: eine fallstudie aus Tall Bazi. Subartu XIX. Brepols Publisher, Turnhout.
Prentice, I.C., Guiot, J., Huntley, B., Jolly, D., Cheddadi, R., 1996. Reconstructing biomes from palaeoecological data: a general method and its application to European pollen data at 0 and 6 ka. Climate Dynamics 12, 185–194.
Reida Sbeinati, M., Darawcheh, R., Mouty, M., 2005. The historical earthquakes of Syria: an analysis of large and moderate earthquakes from 1365 BC to 1900 AD. Annals of Geophysics 48, 347–424.
Reimer, P.J., Baillie, M.G.L., Bard, E., Bayliss, A., Beck, J.W., Bertrand, C.J.H., Blackwell, P.G., Buck, C.E., Burr, G.S., Cutler, K.B., Damon, P.E., Edwards, R.L., Fairbanks, R.G., Friedrich, M., Guilderson, T.P., Hogg, A.G., Hughen, K.A., Kromer, B., McCormac, F.G., Manning, S.W., Bronk Ramsey, C., Reimer, R.W., Remmele, S., Southon, J.R., Stuiver, M., Talamo, S., Taylor, F.W., van der Plicht, J., Weyhenmeyer, C.E., 2004. IntCal04 Terrestrial radiocarbon age calibration, 26–0 ka BP. Radiocarbon 46, 1029–1058.
Reuveny, R., 2007. Climate change-induced migration and violent conflict. Political Geography 26, 656–673.
Schilman, B., Bar-Matthews, M., Almogi-Labin, A., Luz, B., 2001. Global climate instability reflected by Eastern Mediterranean marine records during the Late Holocene. Palaeogeography, Palaeoclimatology, Palaeoecology 176, 157–176.
Schilman, B., Ayalon, A., Bar-Matthews, M., Kagan, E.J., Almogi-Labin, A., 2002. Sea-Land paleoclimate correlation in the Eastern Mediterranean region during the Late Holocene. Israel Journal of Earth Sciences 51, 181–190.
Singer, I., 1999. A political history of Ugarit. In: Watson, W.G.E., Wyatt, N. (Eds.), Handbook of Ugaritic Studies, Handbuch der Orientalistik. Erste Abteilung, Leiden, pp. 603–733.
Singer, I., 2000. New evidence on the end of the Hittite Empire. In: Oren, E.D. (Ed.), The Sea peoples and their World: a reassessment. University of Pennsylvania, Philadelphia, pp. 21–33.
Staubwasser, M., Weiss, H., 2006. Holocene climate and cultural evolution in late prehistoric–early historic West Asia. Quaternary Research 66, 372–387.
Tarasov, P.E., Cheddadi, R., Guiot, J., Bottema, S., Peyron, O., Belmonte, J., Ruiz-Sanchez, V., Saadi, F., Brewer, S., 1998. A method to determine warm and cool steppe biomes from pollen data; application to the Mediterranean and Kazakhstan regions. Journal of Quaternary Science 13, 335–344.
Telford, R.J., Heegaard, E., Birks, H.J.B., 2004. The intercept is a poor estimate of a calibrated radiocarbon age. Holocene 14, 296–298.
Vansteenhuyse, K., 2010. La céramique du chantier A. In: Al-Maqdissi, M., Van Lerberghe, K., Bretschneider, J., Badawi, M. (Eds.), Tell Tweini: onze campagnes de fouilles syro-belges (1999–2010). Documents d'Archéologie Syrienne, Damas. In Print.
Versteegh, G.J.M., 2005. Solar forcing of climate. 2: Evidence from the past. Space Science Reviews 120, 243–286.
Warburton, D., 2003. Love and war in the Later Bronze Age: Egypt and Hatti. In: Metthews, R., Roemer, C. (Eds.), Ancient perspectives on Egypt. University College of London Press, London, pp. 75–100.
Weiss, B., 1982. The decline of the Late Bronze Age civilization as a possible response to climate change. Climatic Change 4, 173–198.
Weiss, H., Bradley, R.S., 2001. What drives societal collapse? Science 291, 609–610.
Weiss, H., Courty, M.A., Wetterstrom, W., Guichard, L., Senior, L., Meadow, R., Curnow, A., 1993. The genesis and collapse of third millennium North Mesopotamian civilization. Science 261, 995–1004.
Whincop, M., 2007. The Iron Age II at Tell Nebi Mend: towards an explanation of ceramic regions. Levant 39, 185–212.
Woolley, G.L., 1958. Alalakh: an account of the excavations at Tell Atchana in the Hatay. Oxford University Press, Oxford.
Yon, M., 1989. The End of the Kingdom of Ugarit. In: Ward, W.A., Sharp Joukowsky, M. (Eds.), The Crisis years: the 12th century BC. From Beyond the Danube to the Tigris. Kendall/Hunt Publishing Company, Dubuque, pp. 111–122.
Yon, M., 2006. The City of Ugarit at Tell Ras Shamra. Hardcover. Eisenbrauns, Winona Lake.